Materials Science in Semiconductor Processing 75 (2018) 157–165

Contents lists available at ScienceDirect

Materials Science in Semiconductor Processing

journal homepage: www.elsevier.com/locate/mssp

Anneal induced transformations of defects in hadron irradiated Si wafers and Schottky diodes

E. Gaubas[a,*], T. Ceponis[a], L. Deveikis[a], D. Meskauskaite[a], J. Pavlov[a], V. Rumbauskas[a], J. Vaitkus[a], M. Moll[b], F. Ravotti[b]

[a] Vilnius University, Institute of Applied Research, Sauletekio ave. 3, LT-10257 Vilnius, Lithuania
[b] CERN, Organisation européenne pour la recherche nucléaire, CH-1211 Genéve 23, Switzerland

ABSTRACT

In this research, the anneal induced transformations of radiation defects have been studied in n-type and p-type CZ and FZ Si samples, irradiated with relativistic protons (24 GeV/c) and pions (300 MeV/c) using particle fluences up to 3×10^{16} cm^{-2}. The temperature dependent carrier trapping lifetime (TDTL) spectroscopy method was combined with measurements of current deep level transient spectroscopy (DLTS) to trace the evolution of the prevailing radiation defects. The contactless TDTL technique has been shown to be preferential when the radiation induced trap density approaches or exceeds the dopant concentration and when it is necessary to avoid modification of a detector structure due to annealing processes at elevated temperatures. The deep level spectra were complementarily examined by using DLTS spectroscopy on Schottky diodes made of irradiated Si wafer fragments. The dominant radiation defects and their transform paths under isothermal and isochronal anneals have been revealed. A good agreement between the DLTS and TDTL spectra has been obtained.

1. Introduction

Silicon based detectors are widely used as particle detectors in experiments of high energy physics [1]. A deep understanding of radiation damage of particle detectors is important in order to extend the sensor lifetime and radiation hardness and potentially to restore their functionality after degradation caused by irradiation. A way to recover detector operational features is heat treatments at technically acceptable temperatures [1–3]. In order to develop adequate annealing procedures and technologies, it is crucial to characterize and understand the evolution of the most harmful radiation induced defects under heat-treatment procedures. Radiation technologies can also be useful for the manipulation of transducer switching rates [4]. However, radiation leads usually to an increase of leakage current and a degradation of barrier features [5]. Combining radiation and annealing technologies could develop into a promising tool for predictable improvements of transducer parameters.

In this work the combined study of radiation defects by deep level transient spectroscopy (DLTS) and temperature-dependent trapping lifetime (TDTL) techniques is used as an effective tool for the identification and tracking of radiation defects in heavily irradiated Si. There, application of standard spectroscopy techniques is limited or impossible due to the extremely high densities of radiation defects significantly exceeding the concentration (N_D) of the shallow dopants. Therefore, the TDTL contactless technique, based on the measurements of the microwave-probed photoconductivity transients (MW-PC), was employed offering the advantage of excluding uncertainties due to the contact quality and disordered diode structure, due to the emerged clusters of radiation defects or even amorphous material regions. The correlation between the DLTS and TDTL spectral signatures enabled us to trace radiation defect transformations in the irradiated Si samples. The deep traps attributed to radiation defects in n-type and p-type Czochralski (CZ) and float-zone (FZ) grown Si were studied on various Si material wafer fragments and detector structures, irradiated with relativistic protons (24 GeV/c) and pions (300 MeV/c) using particle fluences up to $\Phi = 3 \times 10^{16}$ cm^{-2}. Variations of carrier recombination and trapping lifetimes were studied after isothermal anneals at 80 °C, varying heat treatment time from a few to thousands of seconds, and subsequent isochronal heat treatments for 24 h in nitrogen (N_2) ambient by discretely varied temperature from 80 °C to 300 °C. The temperature dependent variations of carrier recombination, trapping and emission lifetime were then measured after each heat treatment procedure. These latter measurements enabled us to compose a spectrum of prevailing radiation defects and to estimate their densities after each

* Corresponding author.
E-mail address: eugenijus.gaubas@ff.vu.lt (E. Gaubas).

https://doi.org/10.1016/j.mssp.2017.11.035
Received 28 September 2017; Received in revised form 23 November 2017; Accepted 24 November 2017

Table 1
Samples and irradiations.

Type of irradiation	Protons (p)		Pions (π^+)	
Relativistic hadrons	24 GeV/c		300 MeV/c	
Fluence range	10^{12}-3 × 10^{16} p/cm^2		10^{11}-3 × 10^{15} π^+/cm^2	
Si material	FZ n-Si	CZ p-Si	CZ n-Si	FZ n-Si
Dopant concentration/ resistivity	10^{12} cm^{-3} > 3 kΩcm	10^{12} cm^{-3} 10 kΩcm	10^{12} cm^{-3} > 3 kΩcm	10^{12} cm^{-3} > 3 kΩcm

anneal step.

2. Experimental techniques and samples

2.1. Samples

Table 1 summarises the used materials and performed irradiations. Two sets of wafer fragments of the CZ (380 μm thick) and float-zone (FZ) grown (280 μm thick) n- and p-type Si of resistivity > 3 kΩcm were irradiated with hadrons. The same irradiated-material wafer fragments were employed for Schottky diode fabrication. The Schottky barrier was formed by 30 nm thick Au evaporated layer on HF freshly-etched wafer top-surface. The ohmic contact was fabricated on the rear wafer side by evaporation of nickel (100 nm). An area of electrodes was set to 3.85 × 10^{-1} cm^2 for these samples to have proper barrier capacitance values and other reasonable parameters for DLTS measurements.

Irradiations by relativistic protons (24 GeV/c) and pions (300 MeV/c) were performed at CERN and at Paul Scherrer Institute in Villigen, respectively, varying fluences in the range of $\Phi_{p,\pi}$ = 10^{11}-3 × 10^{16} cm^{-2}. Fluence is presented as usual by denoting incident particles (protons (p) or pions (π^+)) within a beam cross-sectional area. The relativistic protons and pions induce depth-homogeneous distribution of radiation defects in samples of employed thicknesses, while the used range of fluences covers the actual interval of probable damage sustained by particle detectors in LHC experiments.

The isochronal anneals for 24 h have been performed at the temperatures in the range from 80 °C to 300 °C by temperature steps of 20–50 °C in N_2 gas ambient. The hadron irradiated samples were isothermally annealed at 80 °C up to 5 h before isochronal (24 h) anneals at elevated temperatures. The MCZ (Si grown by CZ with applied magnetic field) material was also examined for comparison of the recombination characteristics in the neutron as-irradiated wafer samples.

2.2. Spectroscopy techniques

2.2.1. DLTS spectroscopy of heavily irradiated samples

Deep level transient spectra over a temperature range of 15–300 K have been recorded on Schottky diode samples by using a HERA-DLTS System 1030 spectrometer [6]. The HERA-DLTS System 1030 spectrometer covers the scan temperature range from 10 to 450 K. The current (I) and optical (O) deep level transient spectroscopy (DLTS) measurements were performed. The DLTS transients were recorded by varying rate windows and using electrical carrier injection pulses of 100 ms duration and 9.9 V amplitude at reverse voltage of 10 V. The capacitance C-(O-)DLTS measurements were only employed for samples irradiated with the lowest fluences. The optical O-DLTS measurements were implemented using IR laser (1064 nm) pulses (of > 10 μs). The measurements and data evaluation were controlled using the PhysTech software installed within the HERA-DLTS System 1030 spectrometer [6].

The barrier capacitance transient, which is determined by the majority carrier emission from deep levels with rate e_n (in n-type material), can be described by the relation

$$\frac{\Delta C(t)}{C} = \begin{cases} -\frac{1}{2}\frac{N_T}{N_{eff}} e^{-e_n t}, & e_n >> e_p \\ 0, & e_n << e_p \end{cases}. \quad (1)$$

Here, $\Delta C(t)$ is the barrier capacitance change due to the emission of carriers from a specific deep level, C is the barrier capacitance value under reverse bias for a fixed voltage, $e_{n,p}$ is the emission rate for electrons and holes, respectively. C-DLTS method is appropriate when the trap concentration N_T is less than 10% of the effective dopant (N_{Deff}) concentration [7–11].

The current deep level transient spectroscopy (I-DLTS) method is preferable [7–11] when it is necessary to overcome limitation concerning effective doping in defect-rich samples. The transient I-DLTS signal of current density δJ (t) is then expressed as

$$\delta J(t) = -\frac{1}{2} q x_d N_T \frac{e_n}{e_n + e_p}(e_n - e_p) e^{-(e_n+e_p)t} = \left\{ \begin{matrix} -\frac{1}{2} q x_d N_T e_n e^{-e_n t} (e_n >> e_p) \\ \frac{1}{2} q x_d N_T e_n e^{-e_p t} \cong 0, (e_n << e_p) \end{matrix} \right\} \quad (2)$$

The amplitude of the transient signal δJ depends on the depletion width x_d, on the concentration N_T of deep traps and on the emission rate e_n. For the rather compensated materials, the optical excitation is commonly employed [7]. In this O-DLTS (Optical injection – DLTS) case, both majority and minority carriers determine the amplitude of the transient signal. The O-DLTS regime ($h\nu \leq E_G$) is close to that employed in photo-induced current transient spectroscopy (PICTS, $h\nu > E_G$) technique where transients are mainly governed by carrier density changes due to thermal emission.

2.2.2. Temperature dependent carrier trapping lifetime technique

Carrier thermal emission parameters can also be examined by the Temperature Dependent Carrier Trapping Lifetime (TDTL) method [12–15]. Contactless measurements of the temperature dependent carrier-trapping lifetime (TDTL) were performed by using a microwave probed photoconductivity transient (MW-PC) technique. The measurements were carried out using pulsed (400 ps) excitation at 1062 nm wavelength and a coaxial needle-tip microwave (22 GHz) probe within a near-field probing regime, performed by a proprietary measuring device VUTEG-6, fabricated at Vilnius University. Our proprietary TDTL instrument covers a scan temperature range from liquid nitrogen (~ 80 K) to 400 K. The combining of the DLTS and TDTL techniques in more detail had been discussed in our previous work [15]. This contactless TDTL technique is preferential when radiation trap density approaches or exceeds the dopant concentration. The two decay processes, recombination and (multi-) trapping-emission, can be distinguished when the two-componential (quasi-two-exponential) transients (Fig. 1(a)) are observed [14,15].

The models of carrier decay processes in the cases of several competing centers were considered in monographs [16,17]. A process of simultaneous recombination and trapping after short pulse excitation with initial (t = 0) excess carrier density $\Delta n(t = 0) = \Delta n_0$ can be described by a set of equations [17]:

$$\frac{\partial \Delta n}{\partial t} = -\frac{\Delta n}{\tau_R} - \frac{\partial \Delta m}{\partial t}, \quad (3A)$$

$$\frac{\partial \Delta m}{\partial t} = \gamma (N_{tr} - \Delta m)\Delta n - \gamma N_{CM} \Delta m, \quad (3B)$$

$$\frac{\partial \Delta p}{\partial t} = -\frac{\Delta p}{\tau_R}, \quad (3C)$$

$$\Delta p(t) = \Delta n(t) + \Delta m(t), \quad (3D)$$

$$\Delta p(t = 0) = \Delta n(t = 0) = \Delta n_0. \quad (3E)$$

Here, Δn, Δm and Δp denote the excess concentrations of free and trapped electrons as well as free excess holes, respectively, γ is the

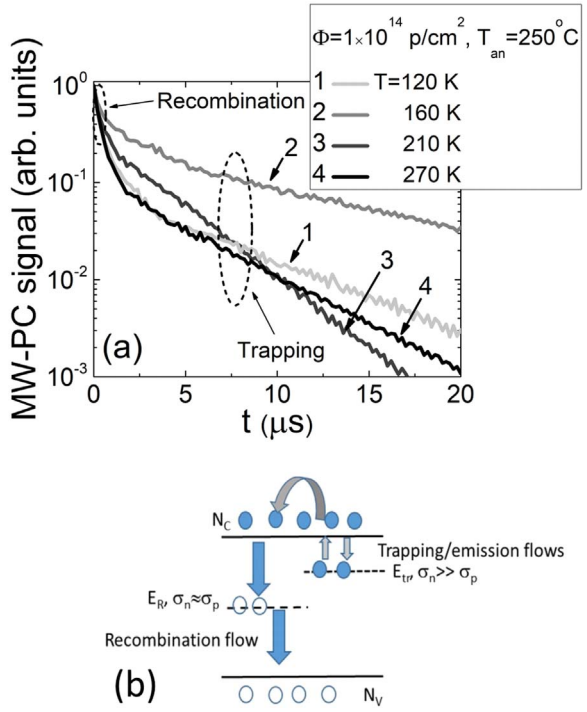

Fig. 1. (a) - The as-recorded MW-PC transients in FZ n-Si samples irradiated with fluence 1×10^{14} p/cm^2 after heat treatment at T_{an} = 250 °C at different scan temperatures (T). (b) – Sketch of simultaneous processes of carrier recombination and trapping.

capture coefficient for electrons, N_{tr} is the concentration of trapping centers with significantly asymmetric capture cross-sections, $N_{CM} = N_{C,V,e,h,Ntr} = N_{C,V} \times exp(-E_{tr}/kT)$ is the effective density of band states for trapped carriers, and $N_{C,V}$ is the density of states in conduction (C) and valence (V) bands, respectively, E_{tr} is the trap activation energy (relative to thermal emission). It is clear that concentration of trapped carriers depends on the concentration of free electrons Δn. Thus, Δm is a function of Δn, i.e. $\Delta m(\Delta n)$. Thereby, Eq. (3A) can be re-written as

$$\frac{\partial \Delta n}{\partial t} = -\frac{\Delta n}{\tau_R} - \frac{\partial \Delta m}{\partial \Delta n}\frac{\partial \Delta n}{\partial t}, \tag{4A}$$

$$\frac{\partial \Delta n}{\partial t}\left(1 + \frac{\partial \Delta m}{\partial \Delta n}\right) = -\frac{\Delta n}{\tau_R}. \tag{4B}$$

Assuming that concentration of trapping centers N_{tr} is arbitrary and the filling of these centers is fast, the conditions of extremal filling and reached steady-state during initial stages of trap filling process can be formulated for the second equation as

$$\frac{\partial^2 \Delta m}{\partial t \partial \Delta n} = 0, \tag{5A}$$

$$\frac{\partial \Delta m}{\partial t}\Big|_{t\approx 0} \cong 0. \tag{5B}$$

The latter conditions lead to relations (using Eq. (5A) and (5B))

$$\frac{\partial \Delta m}{\partial \Delta n} = \frac{N_{tr} N_{CM}}{(\Delta n + N_{CM})^2}, \tag{6A}$$

$$\Delta m \cong \frac{N_{tr} \Delta n}{N_{CM} + \Delta n}, \tag{6B}$$

respectively. Relation (6B) is ascribed to the quasi-steady-state. Then using (6A), Eq. (4) reads

$$\frac{\partial \Delta n}{\partial t}\left(1 + \frac{\partial \Delta m}{\partial \Delta n}\right) \equiv \frac{\partial \Delta n}{\partial t}\left(1 + \frac{N_{tr} N_{CM}}{(\Delta n + N_{CM})^2}\right) = -\frac{\Delta n}{\tau_R}. \tag{7}$$

Eq. (7) is the non-linear equation relative to free carrier concentration and depends on concentration (N_{tr}) and activation energy (E_{tr}, through N_{CM}) of trapping centers. Integral solution of Eq. (7) is represented by a transcendental equation

$$\Delta n(t)\left[\frac{\Delta n(t)}{\Delta n(t) + N_{CM}}\right]^{\frac{N_{tr}}{N_{CM}}} \exp\left[\frac{N_{tr}(\Delta n_0 - \Delta n(t))}{(\Delta n(t) + N_{CM})(\Delta n_0 + N_{CM})}\right] = \Delta n_0 e^{-\frac{t}{\tau_R}}\left[\frac{\Delta n_0}{\Delta n_0 + N_{CM}}\right]^{\frac{N_{tr}}{N_{CM}}}. \tag{8}$$

It can be noticed that Eq. (7) becomes a linear one when $\Delta n > N_{CM}$, N_{tr}. The linearized equation describes a single exponential recombination by $\Delta n(t) = \Delta n_0 \exp(-t/\tau_R)$ for the initial decay stage, where $\Delta n(t) \approx \Delta n_0$ in Eq. (8).

The simulated transients (according to Eq. (8)) are illustrated in Fig. 2. The defects with deep levels and close values of capture cross-sections for both type carriers act as recombination centers. While other centers with considerable difference of capture cross-sections (Fig. 1b) for different carrier types redistribute capture and thermal release flows for one type of carriers. Redistribution of the one type of carrier capture flows between the recombination and trapping centers leads to an asymmetry of trapped and band carrier densities for holes and electrons. Recombination process is as usually fast with a free carrier concentration $\Delta n(t)$ which reduces exponentially with time. Nevertheless, the recombination starts to be governed by trapped carriers Δm when this $\Delta n(t)$ approaches to an effective density of free states for thermally emitted carriers $\Delta m^* \approx N_{CM}$ (Fig. 2a). The non-linearity of the whole decay process, described by Eq. (8), appears within transitional stage $\Delta n_0 < \Delta n(t) < \Delta m^*$ of a transient.

The efficient multi-trapping process is inherent for situations when concentration of traps exceeds the efficient density of states for thermally emitted carriers, i.e. at $N_{tr} > N_{CM}$. This can be explained by fast carrier capture process (due to rather large N_{tr}) and slow carrier (Δm) emission from these traps (due to small density of the final states N_{CM}). Large capture rate ($\gamma \Delta n N_{tr}$) of free carriers determines fast re-trapping of the thermally emitted carriers, thus, leading to the multi-trapping process. While the main part of concentration of excess carriers Δn decays through recombination centers. The thermal emission process becomes dominating when $\Delta n(t)$ decreases to $\Delta n < \Delta m^* \approx N_{CM}$ (Fig. 2a). It can easily be derived (from Eq. (3B) for $\Delta n \approx \Delta m$ and assuming an initial condition $\Delta m = \Delta m^*$) the exponential decay of $\Delta m(t)$ and $\Delta n(t)$ due to thermal emission. Thus, the asymptotic decay, described by Eq. (8), can then be approximated by a single exponent. The instantaneous decay lifetimes (τ_{inst}) have invariable values (Fig. 2c) within initial (τ_R) and asymptotic ($\tau_a = \tau_R(1 + N_{tr}/N_{CM})$) stages of a decay transient. These values are considerably different if $N_{tr} > N_{CM}$, and a two-componential decay is observable. The parameters of trapping centers can be estimated from slopes within initial (τ_R) and asymptotic ($\tau_a = \tau_{inst}|_{t\to\infty}$) stages of transient and by scanning the temperature dependent changes of these lifetimes. For more precise evaluation of the parameters of the emission centers, fitting of transients by Eq. (8) is inevitably applied.

Contrary, for the case of $N_{tr} < N_{CM}$, the density of final states for emitted carriers is large, and this emission process is fast with detrapping lifetime close to that of recombination (Fig. 2d). The recombination process prevails in the latter case. Here, precision of τ_a evaluation is often unacceptable. Thereby, trapping lifetime control, using the TDTL technique, is most efficient for large emission center concentration, in opposite to C-DLTS techniques where requirement of $N_{tr} < N_D$ is essential.

Due to a difference between the carrier recombination (τ_R) and thermal release lifetimes ($\tau_{inst,tr} \approx \tau_R \times [1 + (N_{tr}/N_{C,V}) \times \exp(E_{tr}/kT)]$), carriers captured to the trapping centers delay the recombination process. The two-componential transient approach enables description of the temperature dependent trapping effect at large concentrations of the trapping centers N_{tr}. Then, the instantaneous decay lifetime is expressed through the recombination lifetime (τ_R) and the trapping

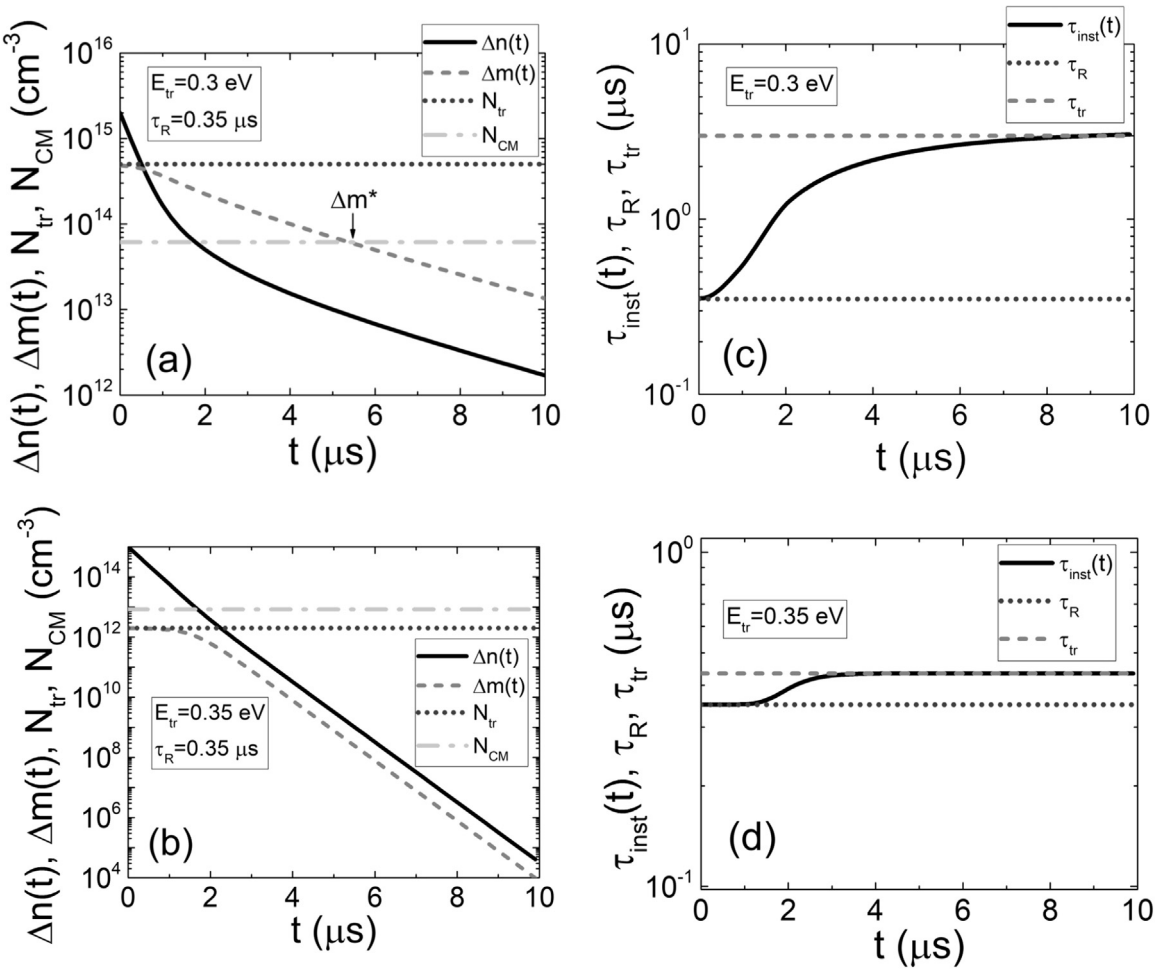

Fig. 2. Simulated (using Eq. (8)) excess carrier $\Delta n(t)$ decay transients (solid lines) are shown on the left panels for efficient multi-trapping process (a) (when long asymptotic decay is determined by carrier trapping and thermal emission from the trapping centers at condition of $N_{tr} > N_{CM}$) and efficient recombination process (b) (for $N_{tr} < N_{CM}$). There, simulated transients of carrier density$\Delta m(t)$ on trapping centers are also illustrated by dashed lines. The horizontal dotted (N_{tr}) and dash-dotted (N_{CM}) lines show concentrations of traps and effective density of states, respectively. On the right panels, the simulated (solid curves) variations (c, d) of the instantaneous decay time linked to the situations of efficient trapping (a, c) and efficient recombination (b, d) are shown, where values of the recombination (dots) and asymptotic trapping (dashes) lifetimes, employed for simulations using Eq. (8), are depicted by the horizontal lines.

coefficient K_{tr} [15] which includes parameters of N_{tr}, $N_{CM}(E_{tr})$ and scan temperature (T) as

$$\tau_{inst,tr} = \tau_R K_{tr}(\Delta n(t, T)); \tag{9A}$$

$$K_{tr}(t, T, T_{an}) = 1 + \frac{N_{tr}(T_{an}) N_{C,V,e,h,Ntr}(T, E_{tr})}{(N_{C,V,e,h,Ntr}(T, E_{tr}) + \Delta n(t, T))^2}; \tag{9B}$$

$$K_{tr}(t, T, T_{an})|_{K_{Tr} >> 1} = \begin{cases} \frac{N_{tr}(T_{an}) N_{C,Ntr}(T, E_{tr})}{(n(t, T))^2}|_{N_{C,Ntr}(T,E_{tr}) < \Delta n(t,T)} \propto T^{3/2} \exp(-E_{tr}/kT), & T < T_{peak} \\ \frac{N_{tr}(T_{an})}{N_{C,Ntr}(T, E_{tr})}|_{N_{C,Ntr}(T,E_{tr}) > \Delta n(t,T)} \propto T^{-3/2} \exp(E_{tr}/kT), & T > T_{peak}, \end{cases} \tag{9C}$$

Here, T is the scan temperature, while T_{an} is the anneal temperature which may cause changes of trap density due to defect transformations. The simulated dependencies of carrier-trapping lifetime (using Eq. (9)) can be applied for spectroscopy of trapping levels, as illustrated in Fig. 3. A peak temperature (T_{peak}), for which the largest trapping coefficient (ascribed to a single type trapping center) is obtained, can be found using condition of extremal trapping coefficient

$$\frac{\partial K_{tr}(T)}{\partial T} = 0. \tag{10A}$$

For fixed excess carrier density Δn_C, the peak temperature (T_{peak}) can be estimated by solving the transcendental equation

$$T_{peak} = A^{2/3} \exp\left(\frac{2}{3}\frac{E_{tr}}{kT_{peak}}\right) \times 300K, \qquad \Delta n_C = const\ . \tag{10B}$$

Here, $A = \Delta n_C / N_{C,V,T\ =\ 300K}$, and $N_{C,V,T\ =\ 300K}$ denotes expression for the density of states $N_{C,V}$ at $T = 300$ K temperature. For varied absorption coefficient $\alpha(T) = \alpha_{300} \times (T/300(K))^{4.25}$ with temperature, concentration of the excess carriers becomes a function of temperature $\Delta n(T) = \alpha(T) \times F$, where $\alpha_{300} = 10\ \mathrm{cm}^{-1}$ [18] is the absorption coefficient for light wavelength 1064 nm in Si at $T = 300$ K, and F is the surface density of incident photons. The peak temperature is then obtained as a real root of the more intricate transcendental equation (relative to (10A)) obtained using a condition of the extremal trapping coefficient.

The pulsed excitation intensity was kept invariable for all the measurements, and an initial density of the excess carriers was simulated to be temperature dependent $\Delta n_0(T)$ due to absorption coefficient changes as a function of temperature. There, peak position can be predicted by Eq. (10A). The necessary re-calibrations of photon surface density (F), adjusted to each scan temperature T in the case of fixed excess carrier density Δn_C (Eq. (10B)), increase the measurement errors (due to an additional set of parameters within evaluations of photon flux per pulse), as was determined from our various TDTL experiments.

A spectrum of TDTL represents the instantaneous trapping lifetime values as a function of scan temperature T or a reciprocal of the thermal

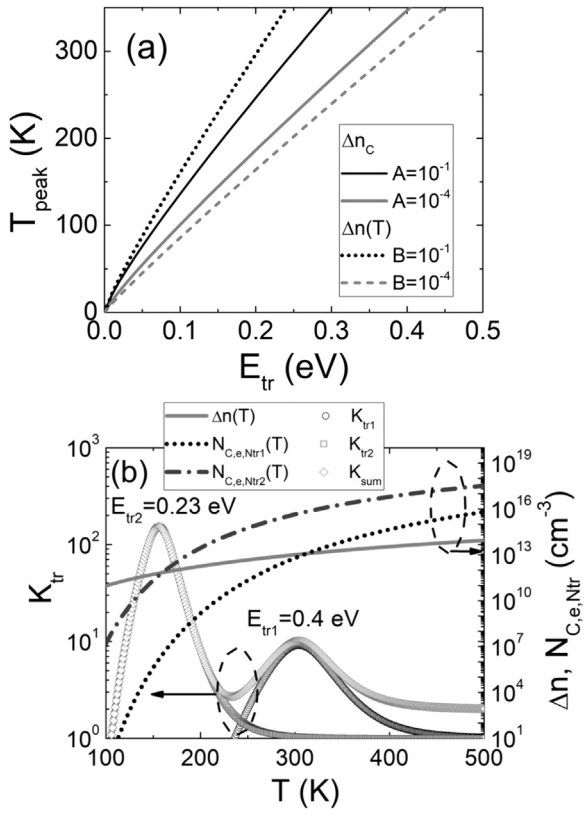

Fig. 3. (a)- Peak temperature (within TDTL spectrum) dependence on trapping center activation energy (E_{tr}) simulated for a fixed $\Delta n_C = const$ and temperature varied $\Delta n_0(T)$ excess carrier density. (b) - Simulated trapping coefficient as a function of scan temperature for the trapping levels with activation energies of 0.4 eV and 0.23 eV and the same N_{tr} (2×10^{14} cm^{-3}) in Si. Here, in (b), temperature dependent variations of the $N_{C,e,Ntr}(T)$ and $\Delta n_0(T)$ are also depicted. Values of $\Delta n_0(T)$ at a fixed excitation intensity might vary due to temperature-dependent changes of the absorption coefficient $\Delta n_0(T) \sim \alpha(T)$ [18].

activation energy ($1/kT$), with k the Boltzmann constant. Only a pair of parameters of the activation energy E_{tr} and trap concentration N_{tr} should be employed as variable parameters within simulation of TDTL spectral peaks, at assumption of fixed cross-section inherent for a definite type of a single-species defect (Fig. 3(b)). There pulsed excitation intensity is kept invariable for all the measurements and density of excess carriers ($\Delta n_0(T,t = 0) = \alpha_{300} \times (T/300)^{4.25} \times F$) is simulated to be temperature dependent $\Delta n_0(T)$ due to absorption coefficient (temperature dependent) changes for a fixed F, according to Eq. (9) and (10), as shown in Fig. 3(b). In analysis of the experimental transients, the Δn_0 and $\Delta n(t)$ are estimated after recombination lifetime evaluation from the initial component of a transient, as $\Delta n(T,t) = \Delta n(T,t = 0) \times exp(-t/\tau_R)$. The effective density of band states $N_{C,V,Ntr}(T,E_{tr})$ should also be incorporated within simulations, while the latter parameter varies only with scan temperature T for a definite E_{tr} value and free carrier band, as shown in Fig. 3(b). However, in practical cases, the TDTL spectral peaks, ascribed to different trapping centers, as usual, overlap (Fig. 3(b)). This leads to complications in interpreting of TDTL spectra.

The TDTL uncertainties, which might appear due to possible variations of temperature dependent cross-section, have been evaluated by examination of DLTS transients dependent on filling pulse duration. For the known deep traps in Si, the temperature dependent variations of capture/emission cross-sections are reported in literature [19]. The possible temperature dependent carrier capture/emission cross-section, attributed to different deep traps, may also slightly change position of spectral peaks, although there is no direct link between peak position and capture cross-section within Eq. (3)–(10), under taken assumptions. To include temperature dependent variations of the cross-sections (additionally to temperature dependent thermal velocity) the ratio of γ_C/γ_{em}, should appear within Eq. (3B) instead of assumption $\gamma_C = \gamma_{em}$ for capture (C) and emission (em) coefficients (cross-sections), respectively.

A limitation of the TDTL technique also appears due to the recombination centers, - the trapping decay component might be hidden when concentrations and capture cross-sections of the recombination centers significantly exceed those of the trapping centers. This is clearly observed in Si samples irradiated with hadrons of the largest fluences of $> 10^{16}$ cm^{-2}, where carrier recombination lifetime is shortened to < 1 ns, and the trapping component is rather weak within MW-PC transients even in the 300 °C annealed samples. Precision of TDTL spectroscopy then decreases. Thus, recombination rate acts as an emission lifetime "scan rate window" (Fig. 3(a)) for TDTL variations similarly to a box-car correlator in DLTS spectroscopy. Nevertheless, existence of trapping component can be easily verified by varying intensity of pulsed excitation and/or by using additional broad-band steady-state bias-illumination, which suppresses action of trapping centers.

3. Results and discussion

The most detrimental defects induced by hadron irradiations seem to be clusters those are fast recombination centers and lead to decrease of charge collection efficiency in Si particles detectors. Heat treatments at elevated temperatures might be a tool for destruction of clusters. An objective of this study was to examine variations of carrier recombination and trapping characteristics and to identify the dominant point traps appeared after partial destruction of clusters, in different type Si materials.

The most significant aspects of carrier recombination and trapping lifetime changes are illustrated below by comparing DLTS and TDTL spectra, recorded on samples irradiated with different particles at several fixed fluences and heat treated at a few fixed temperatures, to highlight tendencies of evolution of emission centers appeared due to partial destruction of clusters. Small variations of spectra caused by intermediate transformations of radiation defects are omitted from discussion not going into particulars. On the other hand, illustrations of spectral variations due to transformations of hadron introduced defects are addressed to demonstrate sensitivity and applicability of the DLTS and TDTL techniques.

3.1. Spectra recorded on n-type FZ and p-type CZ Si irradiated by 24 GeV/c protons

For Si wafer fragments as-irradiated by hadrons, the trapping component within MW-PC transients is not observable. These MW-PC transients are single-exponential for Si materials, as-irradiated by different type hadrons: neutrons, pions, protons. The recombination lifetimes τ_R, evaluated at exp(−1) level, appear nearly independent of technology of high resistivity Si material, while these τ_R values clearly decrease with enhancement of hadron irradiation fluence (Fig. 4). Moreover, nearly the same τ_R values are obtained for a fixed fluence (calibrated to 1 MeV neutron equivalent) value despite of hadron type, i.e. for reactor and spallator neutrons, protons and pions, as illustrated in Fig. 4. Values of carrier lifetimes and their dependencies on hadron irradiation fluence, measured on as-irradiated Si detector structures and wafer samples, actually coincide [20]. Furthermore, these characteristics coincide irrespective of measurement mode, - either just taken from irradiation chamber (Fig. 4a) or during irradiation (Fig. 4b). This result implies that radiation defects initially form the deep levels with similar values of carrier capture cross-sections, acting as pure recombination centers. Heat-treatments using rather low anneal temperatures of 80 °C lead to an appearance of trapping effect which determines a relatively small increase (less than two-times) of recombination lifetime (Fig. 4a), even after long-exposure anneals. This

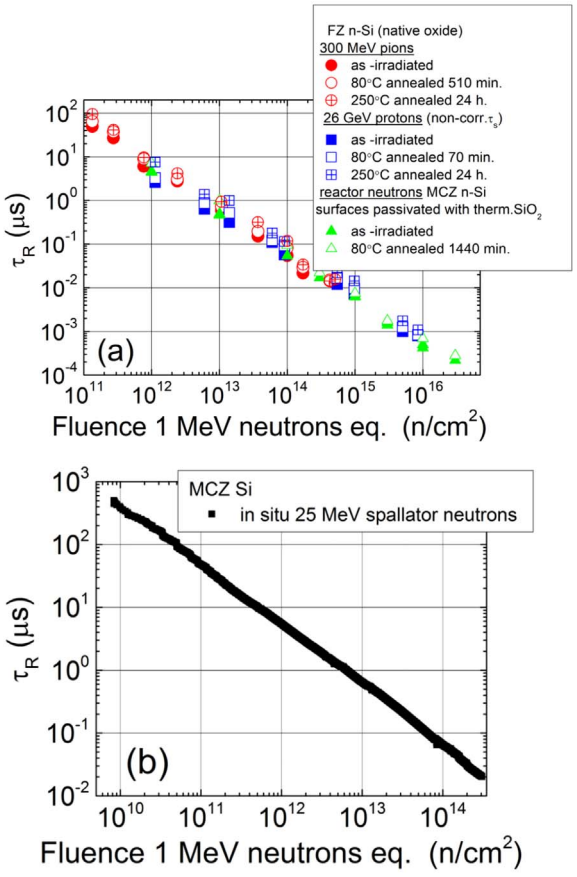

Fig. 4. a – Recombination lifetime in the as-irradiated and annealed Si wafer fragments as a function of fluence of the reactor neutrons, 24 GeV/c protons and 300 MeV/c pions. b – *In situ* variations of recombination lifetime as a function of spallator neutrons. Neutron irradiated MCZ (CZ Si with applied magnetic field) material was also examined.

can be explained by insufficient thermal energy (kT_{an} for T_{an} = 80 °C) to activate transforms of the prevailing radiation defects. The trapping component in the MW-PC transients, caused by competition of several centers in redistribution of carrier capture and thermal emission flows, manifests in samples annealed at elevated temperatures. Moreover, the trapping component becomes the most significant for the annealed samples, those underwent irradiation fluences less than 10^{15} cm^{-2}.

Thus, the temperature scans of trapping lifetime variations allow to examine thermal emission centers ascribed to the dominant point defects (Fig. 5). There, variations of recombination lifetime are rather negligible. In the 24 GeV/c proton irradiated CZ p-Si samples (Fig. 5) using fluences of Φ_p = 1 × 10^{13} and 5 × 10^{13} p/cm^2, the hydrogen (H) and vacancy (V) related complexes have been identified to be responsible for peak formation within deep level spectra [18,21]. After heat-treatments at 200 °C, the dominant peaks with activation energies of 0.17, 0.23, and 0.32 eV have been observed. The activation energies have been extracted by fitting (using Eq. (9)) the experimental TDTL spectra (Fig. 5). The observed TDTL peaks at 1/kT values of 45, 70 and 95 eV^{-1} (Fig. 5) have been attributed to H complexes [21], $V_2^=$ and VO centers, respectively, by comparing with literature data.

The trapping lifetime changes, recorded at different scan temperatures (T) on n-type FZ Si samples, irradiated with fluences of 1 × 10^{14} and 5 × 10^{15} p/cm^2 and heat-treated at 250 °C, are illustrated in Fig. 6. The peaks related to the dominant traps have there been ascribed to A-centers (VO), H related complexes [21], di-vacancies (V_2^- and $V_2^=$) [22–24], and non-identified center with activation energy 0.3 eV. The attribution of traps is denoted in Fig. 6, for different spectral peaks. However, the VO centers have been identified only for the sample, irradiated with fluence of Φ_{pr} = 10^{14} p/cm^2. This can be explained by the

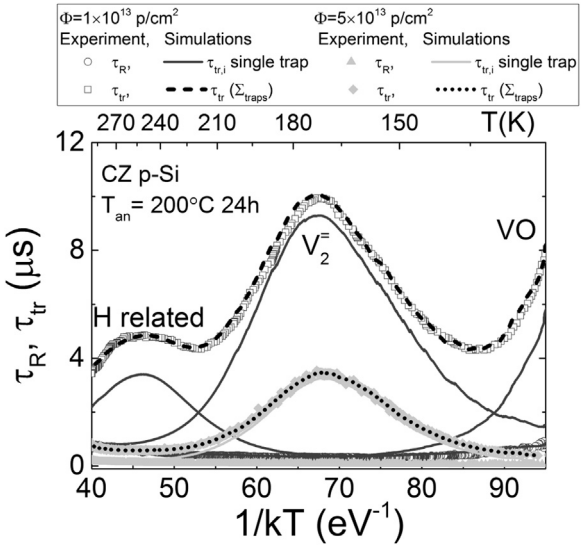

Fig. 5. Comparison of the simulated (curves) and experimental (symbols) variations of the carrier trapping lifetimes τ_{tr} as a function of reciprocal thermal energy kT for p-type CZ Si samples irradiated with fluences 1 × 10^{13} and 5 × 10^{13} p/cm^2 after 200 °C heat-treatment.

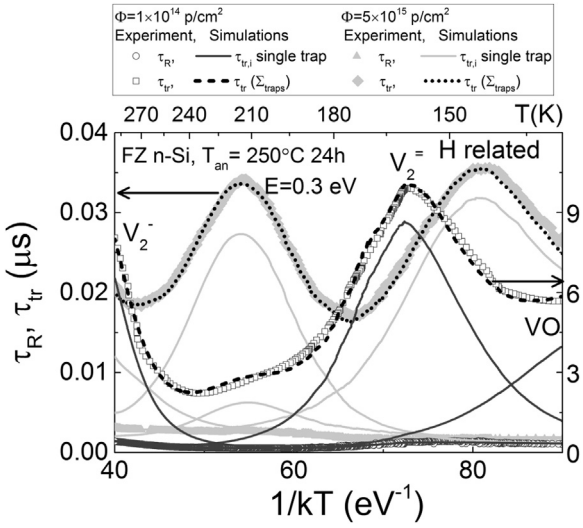

Fig. 6. Comparison of the simulated (curves) and experimental (symbols) variations of the carrier trapping lifetimes τ_{tr} as a function of reciprocal thermal energy for n-type FZ Si samples irradiated with fluences 1 × 10^{14} and 5 × 10^{15} p/cm^2 after 250 °C heat treatment.

considerably lower concentration of oxygen impurities in FZ Si.

Comparison of DLTS spectra, recorded on n-type FZ Si diodes irradiated with 1 × 10^{13} p/cm^2 and 1 × 10^{14} p/cm^2 fluences and annealed at 250 °C, is presented in Fig. 7(a). The predominant peak (150 K) for the sample irradiated with fluence Φ_{pr} = 10^{13} p/cm^2 is attributed to H related defects (E_{tr} = 0.32 eV). While, spectral peaks, observed at 220 K (0.42 eV) and 260 K (0.57 eV), are attributed to di-vacancy (V_2^-) and vacancy related defects. The spectral peaks at 80 K (E_{tr} = 0.2 eV) and 40 K (0.15 eV) within the lower temperature wing are attributed to H related defects and thermal donors (TD), respectively. In samples irradiated using the higher fluence Φ_{pr} = 10^{14} p/cm^2, the predominant peak is attributed to di-vacancy $V_2^=$ (E_{tr} = 0.23 eV). The additional peak obtained at the 60 K is attributed to A-centers. Moreover, an increase of the amplitudes of the peaks at 80 K, 60 K and 40 K has been observed. These DLTS results are in qualitative agreement with TDTL results (Fig. 6) obtained for samples irradiated using the elevated fluences.

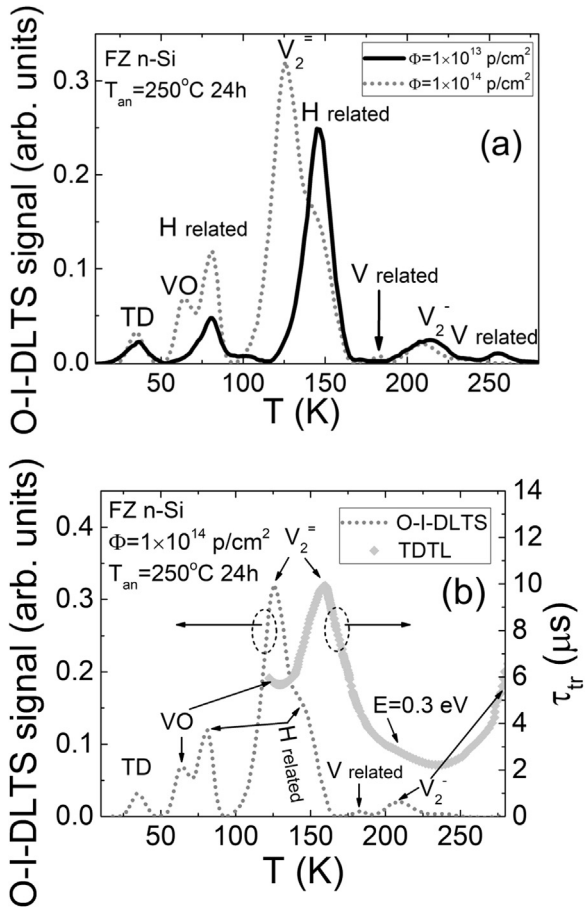

Fig. 7. a – O-I-DLTS spectra recorded on n-type FZ Si diodes irradiated with 1×10^{13} p/cm^2 and 1×10^{14} p/cm^2 fluences and annealed at 250 °C. b – Comparison of the TDTL and O-I-DLTS spectra recorded on n-type FZ Si material irradiated with protons of 1×10^{14} p/cm^2 fluence and annealed at 250 °C.

The combining of the TDTL and DLTS techniques has been applied for benchmarking the TDTL spectroscopy and verification of the origin of a definite-type single-species trapping center. Activation energy values are rather standardized and tabulated for identification of the origin of the definite-type single-species emission centers in DLTS nomenclature of the radiation defects in Si materials of different technology.

Comparison of the TDTL and O-I-DLTS spectra recorded on n-type FZ Si material irradiated with protons of 1×10^{14} p/cm^2 fluence and annealed at 250 °C is illustrated in Fig. 7(b). It is clear that the peak positions relative to the temperature scale should be rather different within recorded TDTL and O-I-DLTS spectra due to different measurement conditions (of excitation pulse duration, e.g. 400 ps for TDTL and > 10 μs for O-I-DLTS; of rate windows -τ_R ~ 1–1000 ns for TDTL, and f ~ kHz for O-I-DLTS; and so on). The range of scan temperatures is also different due to cryogenic systems of the TDTL and DLTS spectrometers. Nevertheless, the origin of the prevailing TDTL defects ascribed to a definite range of scan temperatures is in agreement with DLTS determined traps. Fortunately, the O-I-DLTS spectrometer allows to cover the wider range of *T*'s and thereby to trace anneal dependent evolution of the shallower traps. On the other hand, necessity of contacts and barriers for DLTS samples also introduces uncertainties in comparison of the TDTL and DLTS spectra due to modification of material by technological procedures as well as of quality of the contacts and barriers by irradiations. Thus, the TDTL technique can be suitable for spectroscopy of emission centers and for separation of the recombination and trapping centers when C-DLTS as well as I-DLTS do not longer work properly or evaluation of recombination centers is impossible. The direct coincidence of the TDTL and DLTS parameters is actually impossible, due to possible differences in samples and measurement conditions. Therefore, the qualitative agreement between TDTL and DLTS could be considered which means that the structure of the emission trap spectrum (nature of the prevailing centers and temperature range of their appearance coincides) and anneal dependent changes of partial peak amplitudes (roughly proportional to trap concentration) correlate. In this sense, the TDTL spectroscopy is a reliable tool for tracing of the radiation defect evolution for the range of elevated fluences, where applications of the traditional DLTS is limited.

3.2. Trapping lifetime spectra for n-type FZ and CZ Si irradiated by 300 MeV/c pions

The dominant defects in n-type FZ Si, induced by pion irradiations and subsequent heat treatments using 150 °C anneal temperature, have been ascribed to di-vacancies (V_2^- and $V_2^=$) and to VO complexes, as deduced using TDTL spectroscopy (Fig. 8). While for the CZ Si samples processed using the same procedures, the predominant defects are $V_2^=$ and C_iC_s complexes [22–24]. After subsequent heat treatment using 250 °C temperature anneals (Fig. 9), the $V_2^=$ and VO defects become predominant in FZ and CZ Si. It has been deduced from Fig. 9 that C_iC_s complex anneals out in CZ Si samples, irradiated with $\Phi_\pi = 1 \times 10^{14}$ π^+/cm^2. There, the V_2 complex and the unidentified defect with activation energy $E_{tr} = 0.3$ eV have been observed in FZ n-Si samples.

It has been revealed from DLTS spectroscopy (Fig. 10), performed on samples irradiated with rather small pion fluences, that VO, double charged di-vacancy ($V_2^=$), H-related and V-related defects [21] are dominant in CZ n-Si samples after heat treatment at 250 °C. While, the thermodonors (TD) and negatively single-charged di-vacancy (V_2^-) defects are dominant in the FZ n-Si samples. Concentrations of these defects, which are proportional to the obtained peak amplitudes in DLTS spectra, indicate that production of radiation defects is less efficient for FZ Si, in the examined spectra.

In this aspect, it can be assumed the elevated radiation hardness of FZ Si material relative to CZ one, however, MCZ material (Fig. 4) as usually shows the biggest radiation hardness owing to rather high density of oxygen impurities and rather low concentration of other defects. The lower concentrations of radiation defects in FZ Si can be explained assuming the less density of nucleation centers in production of complexes with radiation defects, due to the considerably lower

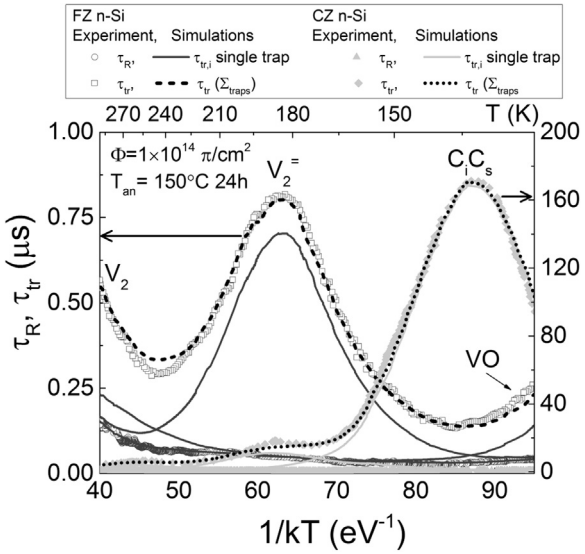

Fig. 8. Comparison of the simulated (curves) and experimental (symbols) variations of the carrier trapping lifetime τ_{tr} as a function of reciprocal thermal energy for n-type FZ and CZ Si samples irradiated with fluence $\Phi_\pi = 1 \times 10^{14}$ π^+/cm^2 and heat-treated at 150 °C.

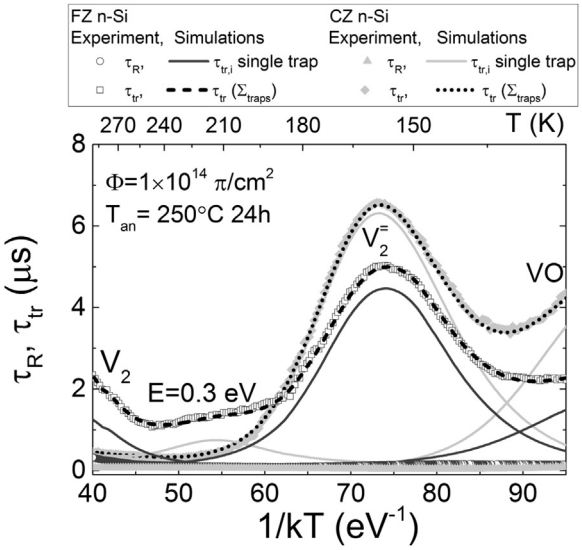

Fig. 9. Comparison of the simulated (curves) and experimental (symbols) variations of the carrier trapping lifetimes τ_{tr} as a function of reciprocal thermal energy for n-type FZ and CZ Si samples irradiated with fluence $\Phi_{\pi} = 1 \times 10^{14}\ \pi^{+}/cm^{2}$ after heat treatment at 250 °C.

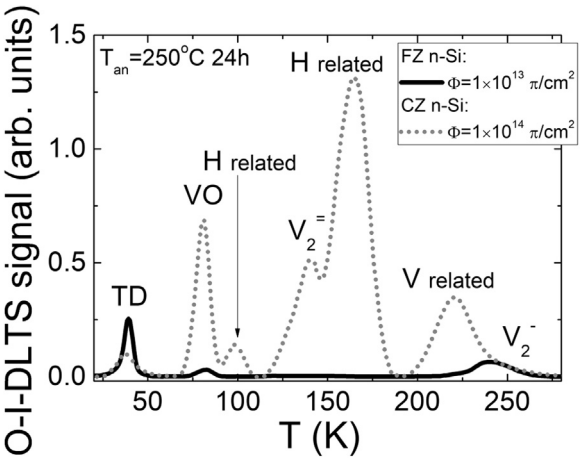

Fig. 10. O-I-DLTS spectra recorded on n-Si samples of FZ material, irradiated with $1 \times 10^{13}\ \pi^{+}/cm^{2}$ fluence, and CZ material, irradiated with $\Phi_{\pi} = 1 \times 10^{14}\ \pi^{+}/cm^{2}$ fluence, and subsequently heat-treated at 250 °C.

concentration of the contaminant impurities and grown-in defects within FZ Si.

The revealed spectra of point defects and their variations after heat treatments, using elevated temperatures, imply dissociation of radiation clusters, those prevail in the hadron as-irradiated material. However, the density of the heat-treatment produced point defects increases and the type of prevailing emission centers varies with anneal steps. These variations also depend on the pristine material and irradiation fluence.

3.3. Generalization

The parameters of traps introduced by irradiation of relativistic protons and pions of nearly the same fluence are listed in Tables 2 and 3, respectively.

The non-monotonous variations of trap densities after different anneal steps can be deduced from Tables 2 and 3. Application of the TDTL technique allowed to identify the trapping centers appeared after heat treatment at $T_{an} \geq 80$ °C. For the hadron (both, protons and pions) irradiated samples, the DLTS peaks ascribed to the oxygen, vacancy and hydrogen (H) related complexes and to thermodonors (TD) have been identified for the n-type CZ and FZ Si samples after annealing for 24 h at 250 °C. The similarity between DLTS spectra, obtained for rather low fluence irradiations by protons and pions, indicate that the irradiation with various type penetrative hadrons induce the same defects. Nevertheless, irradiations with pions lead to introduction of the VO, di-vacancy ($V_2^{=}$), H-related and V-related complexes which are dominant in the n-type CZ Si samples. While, thermodonors (TD) and di-vacancy (V_2^{-}) defects are dominant in the n-type FZ Si samples. The amplitudes of peaks within DLTS and TDTL spectra, recorded on samples irradiated with the same fluence, indicate that the production of radiation defects is less efficient in FZ Si, due to the lower concentration of the contaminants and grown-in defects in comparison with CZ Si.

The TDTL measurements showed the spectral changes dependent on irradiation type (either protons or pions). For p-type CZ and n-type FZ Si samples irradiated with protons, the TDTL spectral peaks have been ascribed to di-vacancies (V_2^{-}, $V_2^{=}$ and V_2^{+}), VO and H related defects. The vacancy ascribed and H-related defects are inherent radiation defects introduced by protons, rather high concentrations of which appear as a result of destruction of radiation clusters under heat treatments. Their density increases with anneal temperature actually due to enhancement of defect activation energy with heat-treatment temperature. The interstitial-substitutional carbon (C_iC_s) complexes have been revealed to be the predominant defect in pion irradiated CZ n-Si material after heat treatment at 150 °C, as carbon impurities of concentration $> 10^{16}\ cm^{-3}$ and oxygen impurities of $> 10^{18}\ cm^{-3}$ are present in the pristine Si material. However, in the hadron irradiated material, anneal induced transformations of cluster defects lead to predominance of C_iC_s complexes in CZ Si at intermediate heat treatment temperatures of 150 C. Formation of VO centers in FZ Si is also probable, where concentration of oxygen impurities of $\sim 10^{16}\ cm^{-3}$ is sufficient to observe VO traps after intermediate heat treatment at 150 C. The subsequent annealing out of the C_iC_s traps is accompanied by formation of the non-identified defect with activation energy $E_{tr} = 0.3$ eV. The latter point defect is also inherent for electron irradiated Si [15].

Carrier recombination lifetime shows a clear tendency of linear decrease in log-log scale (Fig. 4), due to increase of the density of cluster defects (N_{cl}) with fluence of hadrons. Assuming the same rate of cluster destruction by heat treatments, the ratio of point defect density to that of clusters decreases with enhancement of fluence. Thus, the amplitude of trapping component is also reduced for heavily irradiated and annealed samples, and sensitivity of TDTL technique (for I-O-DLTS,

Table 2
Anneal dependent variation of parameters of trapping centers introduced by 24 GeV/c protons.

Activation energy (eV)	Defect identification [reference]	Heat-treatment Sample material	100 °C	150 °C	200 °C	250 °C
			$\Phi = 5 \times 10^{13}$ p/cm^2 Concentration of trapping centers (10^{13} cm^{-3})			
0.32 ± 0.02	H-related [21]	CZ p-Si	7	15	10	220
0.36 ± 0.02	V_2^0 [21]	FZ n-Si	2	11	6	660
0.25 ± 0.01	$V_2^=$ [21]	CZ p-Si	8	12	14	160
		FZ n-Si	8	9	10	180
0.18 ± 0.01	VO [21]	CZ p-Si	0.5	1	1.2	20
		FZ n-Si	0.5	1	1.6	7

Table 3
Anneal dependent variation of parameters of trapping centers introduced by 300 MeV/c pions.

Activation energy (eV)	Defect identification [reference]	Heat-treatment Sample material	Annealed at 100 °C $\Phi = 3 \times 10^{13}\ \pi^+/cm^2$ Concentration of trapping centers ($10^{13}\ cm^{-3}$)	at 150 °C	at 200 °C	at 250 °C
0.36 ± 0.02	V_2^0 [21]	CZ n-Si	8	13	25	5
		FZ n-Si	2	6	12	20
0.25 ± 0.01	$V_2^=$ [21]	CZ n-Si	7	15	20	20
		FZ n-Si	2	7	14	18
0.18 ± 0.01	VO [21]	CZ n-Si	0.2	0.2	0.2	0.6
		FZ n-Si	0.4	0.7	0.8	1

as well) to resolve spectra of emission centers falls down with increase of fluence (Eq. (9A), Fig. 3b, as $\tau_{inst,tr} \approx \tau_R \times (N_{tr}/N_{C,V}) \times \exp(E_{tr}/kT)|_{Ktr>1, Ntr/Ncl<1} \sim N_{tr}/N_{cl} \sim \tau_R$ even for $t \to \infty$). Heat treatment induced transformations and reactions of point radiation defects (for instance, V →V_2, VO) with technological ones lead to intricate changes of TDTL spectra dependent on Si material type (Table 2, when comparing densities of different type defects), anneal temperature (Tables 2 and 3) and heating regime (isothermal, – Fig. 4a, and isochronal, Figs. 5, 6, 8), as well as on irradiation fluence (e.g., when comparing of spectra in Figs. 5 and 6). Nevertheless, a clear tendency of cluster (acting as recombination centers) destruction and consequent formation of emission (trapping) ones with enhancement of isochronal anneal temperature can be deduced from Tables 2 and 3. While, different shape functions (increasing, non-monotonous, saturating) can be implied from Tables 2 and 3 for anneal induced variations of the density of various species emission centers, identified for a fixed irradiation fluence.

4. Summary

The prevailing point traps, which appear after thermal destruction of radiation clusters, have been identified. It has been shown that these point defects mainly act as the efficient thermal emission centers.

Different species of traps and paths of their transformations under anneals have been identified in silicon irradiated with hadron fluences of wide range by combining the DLTS and TDTL spectroscopy.

It has been demonstrated that contactless spectroscopy of carrier recombination and trapping lifetime using MW-PC and TDTL temperature scans allows simultaneous control of interactions among several radiation defects within large fluence irradiated Si structures. This technique is promising for spectroscopy of radiation defects when the standard contact methods become unsuitable due to the disordered structures and internal electric fields existing within heavily radiation damaged materials. It has been proved that TDTL technique is the most efficient for characterization of emission centers with large concentration N_{tr}, inherent for heavily irradiated materials, in opposite to C-DLTS techniques where requirement of $N_{tr} < N_D$ is essential. The increase of concentration of the emission centers in heat-treated samples, which leads to appearance of the two-componential carrier decay transients, implies dissociation of the extended radiation defects those act as prevailing recombination centers in the hadron as-irradiated Si materials.

Acknowledgments

This research was implemented according to AIDA-2020 grant. This study was partially supported by Lithuanian Academy of Sciences, grants LMA-CERN-2016/2017. Paul Scherrer Institute, Villigen, Switzerland and the support provided by T.Rohe, M.Glaser and K.Deiters for performing the irradiations. The work was partly performed in the framework of the CERN RD50 collaboration.

References

[1] H. Spieler, Semiconductor Detector Systems, Oxford University Press, New York, 2005.
[2] Experiments at CERN. ⟨https://home.cern/about/experiments⟩ (accessed 20 September 2017).
[3] Zh Li, E. Verbitskaya, V. Eremin, A. Ivanov, J. Härkönen, E. Tuovinen, P. Luukka, Detector recovery/improvement via elevated-temperature-annealing (drive)-a new approach for Si detector applications in high radiation environment in SLHC, IEEE Trans. Nucl. Sci. 53 (2006) 1551–1556.
[4] E. Gaubas, T. Ceponis, A. Uleckas, J. Vaitkus, Recombination characteristics in 2–3 MeV protons irradiated FZ Si, Nucl. Instr. Meth. Phys. Res. A 612 (2010) 559–562.
[5] E. Gaubas, T. Ceponis, S. Sakalauskas, A. Uleckas, A. Velička, Fluence dependent variations of barrier charging and generation currents in neutron and proton irradiated Si particle detectors, Lith. J. Phys. 51 (2011) 230–236.
[6] FT 1030 Deep-Level Transient Spectroscopy System. ⟨http://www.phystech.de/products/dlts/dlts.htm⟩ (accessed 13 September 2017).
[7] D.V. Lang, Deep-level transient spectroscopy: a new method to characterize traps in semiconductors, J. Appl. Phys. 45 (1974) 3023–3032.
[8] P. Blood, J.W. Orton, The Electrical Characterization of Semiconductors: majority Carriers and Electron States, Academic Press Inc, San Diego, 1992.
[9] S.U. Pandey, P. Middelkamp, Z. Li, V. Eremin, New experimental and analysis methods in I-DLTS, Nucl. Instrum. Meth. Phys. Res. A 426 (1999) 109–113.
[10] E. Gaubas, D. Bajarūnas, T. Čeponis, D. Meškauskaitė, J. Pavlov, Optically induced current deep level spectroscopy of radiation defects in neutron irradiated Si pad detectors, Lith. J. Phys. 53 (2013) 215–218.
[11] C. Hurtes, M. Boulou, A. Mitonneau, D. Bois, Deep-level spectroscopy in high--resistivity materials, Appl. Phys. Lett. 32 (1978) 821–823.
[12] E. Gaubas, T. Čeponis, A. Uleckas, J. Vaitkus, Anneal dependent variations of recombination and generation lifetime in neutron irradiated MCZ Si, Nucl. Instrum. Meth. Phys. Res. A 612 (2010) 563–565.
[13] E. Gaubas, T. Čeponis, J. Pavlov, A. Velička, V. Kalesinskas, Spectroscopy of radiation traps in Si by temperature dependent photoconductivity and generation currents, Lith. J. Phys. 54 (2014) 89–93.
[14] E. Gaubas, E. Simoen, J. Vanhellemont, Review-carrier lifetime spectroscopy for defect characterization in semiconductor materials and devices, ECS J. Solid State Sci. Tech. 5 (2016) 3108–3137.
[15] V. Rumbauskas, D. Meskauskaite, T. Ceponis, E. Gaubas, Anneal induced transforms of radiation defects in heavily electron irradiated Si diodes, J. Instrum. 11 (2016) P09004.
[16] A. Rose, Concepts in Photoconductivy and Allied Problems, Intersciencz Publishers, New York, 1963.
[17] S.M. Ryvkin, Photoelectric Effects in Semiconductors, Consultants Bureau, New York, 1964.
[18] N.G. Nilsson, K.G. Svantesson, The role of free carrier absorption in laser annealing of silicon at 1.06 μm, J. Phys. D: Appl. Phys. 13 (1980) 39–44.
[19] B.S. Avset, Measurements on a hole trap in neutron-irradiated silicon, Nucl. Instrum. Meth. Phys. Res. A388 (1997) 361.
[20] E. Gaubas, A. Kadys, A. Uleckas, J. Vaitkus, Investigation of carrier recombination in Si heavily irradiated by neutrons, Acta Phys, Polonica 113 (2008) 829.
[21] M.L. David, E. Oliviero, C. Blanchard, J.F. Barbot, Generation of defects induced by MeV proton implantation in silicon – Influence of nuclear losses, Nucl. Instrum. Meth. Phys. B 186 (2002) 309–312.
[22] M. Bruzzi, et al., Thermal donors formation via isothermal annealing in magnetic Czochralski high resistivity silicon, J. Appl. Phys. 99 (2006) 093706.
[23] N. Ganagona, L. Vines, E.V. Monakhov, B.G. Svensson, Formation kinetics of trivacancy-oxygen pairs in silicon, J. Appl. Phys. 116 (2014) 124510.
[24] I. Pintilie, E. Fretwurst, G. Lindström, Cluster related hole traps with enhanced-field-emission - the source for long term annealing in hadron irradiated Si diodes, Appl. Phys. Lett. 92 (2008) 024101.